International Journal of Modern Physics E
Vol. 31, No. 3 (2022) 2250032 (9 pages)

DOI: 10.1142/S021830132250032X

World Scientific
www.worldscientific.com

Energy transitions and half-life determinations of ^{47}Sc isotopes from photonuclear reaction on Ti target

Gökhan Koçak*,¶, Serkan Akkoyun†, İsmail Boztosun‡ and Haris Dapo§

*Department of Physics, Faculty of Sciences, Erciyes University, Kayseri, Turkey

†Department of Physics, Faculty of Science, Sivas Cumhuriyet University, Sivas, Turkey

‡Department of Physics, Faculty of Science, Akdeniz University, Antalya, Turkey

§Institute of Accelerator Technologies, Ankara University, Ankara, Turkey
¶gkocak@erciyes.edu.tr

Received 17 November 2021
Revised 18 February 2022
Accepted 18 February 2022
Published 7 April 2022

For the activation of the target nucleus, bremsstrahlung photons generated in a medical linear accelerator can be used. Due to particle separation energy limitations for low photon energies in the giant resonance region (∼18 MeV), the reaction exit channels are restricted to the ejection of one or two particles only. Thus, the gamma spectrum is relatively clear, and the use of ancillary detectors coupled to HPGe is not highly needed. In this study, the bremsstrahlung photons have been used for the activation of the titanium target. $^{46-48}$Sc isotopes are observed from the natural titanium target via photo-proton reactions. Decay radiations from the isotopes and half-life of ^{47}Sc which is from the most abundant natural titanium have been determined consistent with the literature values.

Keywords: Photonuclear reaction; energy transition; half-life; titanium; bremsstrahlung.

PACS Number(s): 25.20.−x, 23.20.Nx, 25.20.Dc

1. Introduction

The ejection of protons, neutrons or light particles from the nucleus accompanying the activation of a target by photons is called a photonuclear reaction. If the photonuclear reaction involves the ejection of one or more nucleons by the target nucleus, then the nucleus created ends up in an excited state and needs to emit a

¶Corresponding author.

particle or gamma-rays to get rid of its excess energy. In the offline analysis, owing to almost all nuclear-excited states being very short (in the order of ∼ps), seeing these prompt gamma-rays arising from exciting nuclei immediately after ejecting nucleons in the photonuclear reaction is unexpected. On the other hand, if the nucleus created by the photonuclear reaction has resulted in unstable radionuclides then it can decay via particle emission to another stable nucleus most commonly via beta decay. If the beta-decay half-life of the produced radionuclide is long enough for offline analysis, the characteristic gamma-rays accompanying the beta-decay can be observed in the spectrum.

The above-mentioned reactions play an important role in various fields of nuclear physics studies,[1–3] for instance, the studies of neutron binding energy, identification of nuclear energy levels and nuclear deformations and half-life of the unstable isotopes. Furthermore, the photonuclear reactions are also important for the generation of medical radioisotopes, application of radiation protection, dosimetry, calculation of absorbed dose, designing radiation shielding and activation analyses.

In the giant dipole resonance region (about 15–30 MeV), photonuclear reaction cross-sections are quite large. The experimental studies on these reactions began in 1934,[4] but the data in the literature are still incomplete. Therefore, additional studies related to photonuclear reactions on different target materials with different energies are needed. Determination of the multiple elements simultaneously, nondestructive structure of the process, requiring no time-consuming chemical separation procedure, deeper penetrating capability of the photon into the target are some of the advantages of the photonuclear reactions.[5–10]

In this study, the photon-activation method has been used in order to determine the photonuclear reaction products of titanium nuclei in its natural isotopic mixture. A mixture of titanium isotopes contains five isotopes with the natural abundances of 8.25% ^{46}Ti, 7.44% ^{47}Ti, 73.72% ^{48}Ti, 5.41% ^{49}Ti and 5.18% ^{50}Ti. Previous experimental investigations into the photodisintegration of titanium isotopes are presented in Refs. 11–17. According to the results, the main product is ^{47}Sc from the most abundant titanium isotope via photo-proton reaction. This isotope can be generated via different ways and is very important for medical applications both in treatment and imaging.[18,19] The other products generated in the reaction are ^{46,48}Sc isotopes which contribute to the gamma-ray spectrum.

The paper is organized as follows: in Sec. 2, we give the details of the experiment and data analysis used in this study. The results and discussions are provided in Sec. 3 and finally, we present our conclusions in Sec. 4.

2. Experiment and Data Analysis

In this study, we have performed the photonuclear reaction experiment by bombarding natural titanium target with high energy bremsstrahlung photons. The clinical linear accelerator (linac) is able to provide photons in sufficient numbers for the

reaction.[20–29] Elekta Synergy medical linac has been used for the generating of the photons. The primary electron beam with 50 keV energy is accelerated through a copper cavity by 3 GHz radio frequency with about 5 MW peak power. The average electron current as stated by the manufacturer should be about 30 μA at the electron energy of 18 MeV. The electrons were stopped by hitting the tungsten target. By slowing down the electrons, bremsstrahlung photons were produced with 18 MeV maximum energy. The resulting photon beam is shaped to a spatially flat profile by using flattening and collimating filters. Since the exact flux and energy profile of the electron beam falling onto the tungsten are not certain and given the influence of the collimator which absorbs up to 80% of the photons the exact energy profile of the photon beam is impossible to know.

As stated before, the target was a natural mixture of titanium isotopes containing five isotopes with the natural abundances of 8.25% ^{46}Ti, 7.44% ^{47}Ti, 73.72% ^{48}Ti, 5.41% ^{49}Ti and 5.18% ^{50}Ti and was used as a target material. The target was placed 58 cm away from the photon source. The total irradiation time was 1 h. Only one neutron and one proton separation energies are below the 18 MeV energy threshold.

In order to understand which reactions to expect after activation we have to look at the relevant proton and neutron separation energies from the titanium target (Table 1). The ejection of higher nucleon numbers or different particle types is not possible in this experiment. Therefore, we only expect to see (γ, n) and (γ, p) reaction products leading to ^{45}Ti, ^{46}Ti, ^{47}Ti, ^{48}Ti, ^{49}Ti, ^{45}Sc, ^{46}Sc, ^{47}Sc, ^{48}Sc and ^{49}Sc isotopes. The reaction paths that are possible can be traced in Segre plot whose part is given in Fig. 1.

In the offline analysis, it is not possible to see prompt gamma-rays from products which end in stable nuclei. Therefore, the gamma-rays from the transitions in $^{45-49}$Ti created via photo-neutron reactions and $^{45-49}$Sc from photo-proton reactions are not expected to be seen in the gamma-ray spectrum. All possible reactions observed in this study have been given in Sec. 3.

After the irradiation process, the residual activity of the target has been measured by an HPGe (AMATEK-ORTEC (GEN40P4-83)) detector. It is a p-type coaxial detector with an electrical cooling system. The relative efficiency is 40% and the full-width at half-maximum is 1.85 keV for energy values of 1332 keV. The detector is connected to bias supply, amplifier, analog-to-digital converter and a

Table 1. Energy thresholds for one neutron and one proton separation reactions after gamma irradiation.

Isotope	(γ, n) threshold in keV	(γ, p) threshold in keV
^{46}Ti	13,189.3	10,344.9
^{47}Ti	8880.88	10,465.1
^{48}Ti	11,626.66	11,445.1
^{49}Ti	8142.40	11,349
^{50}Ti	10,939.19	12,159

^{45}Ti 184.8 min β^+	**^{46}Ti** **8.0%**	**^{47}Ti** **7.3%**	**^{48}Ti** **73.8%**	**^{49}Ti** **5.5%**	**^{50}Ti** **5.4%**	^{51}Ti 5.76 min β^-
^{44}Sc 3.9 h, 59 h β^+, IT	**^{45}Sc** **100%**	^{46}Sc 83.8 day, 19 s β^-, IT	^{47}Sc 3.3492 day β^-	^{48}Sc 43.67 h β^-	^{49}Sc 57.2 min β^-	^{50}Sc 102.5 s β^-

Fig. 1. A part of Segre chart. The stable titanium and scandium isotopes are shown in black color. The half-lives and decay modes are indicated for each radioisotope inside the boxes.

computer. The detector is placed in a lead shield with 10 cm thickness. In order to protect the detector from X-rays arising in lead, the inner surface of the shield is covered by 2 mm copper foil. The standard calibration sources of ^{22}Na, ^{54}Mn, ^{133}Ba, ^{137}Cs, ^{57}Co and ^{60}Co have been used for energy calibration. The total counting time was about 74.3 h. The gamma-ray spectrum measured by HPGe has been shown in Fig. 2.

The MAESTRO software was used to collect the data. The RadWare program created for analyzing gamma-ray coincidence data[30] was used to analyze the peaks. Energy calibration was performed in ROOT.[31] The goal of employing two distinct programs was to find a compromise between the needed accuracy and the amount of time it took to analyze the data. Finally, the information was compiled into a simple calculation sheet that provided the transition-energy value as well as the accompanying error. The RadWare package was used to evaluate all recorded sample and background spectra, as well as calibration spectra taken before and after the experiment. We computed the centroids, areas and related statistical errors of all peaks identified in a spectrum by applying a Gaussian, a skewed Gaussian, and a smoothed step function to any number of chosen peaks.

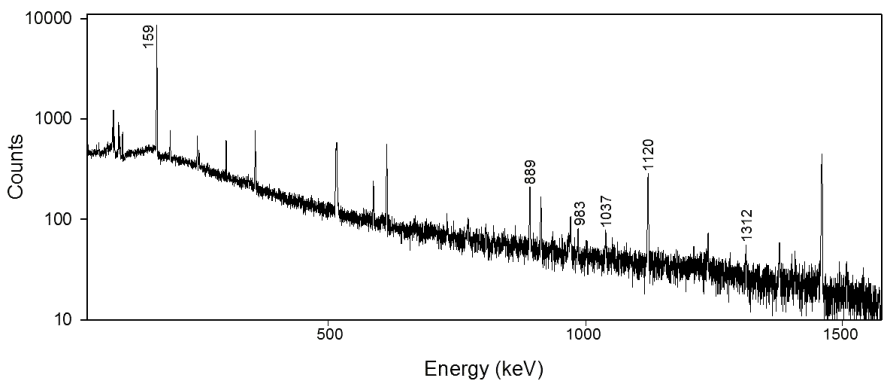

Fig. 2. Gamma-ray spectrum for irradiated titanium sample measured by the HPGe detector.

The calibration data collected before and after the experiment were used in the first step of the study. We were able to determine the calibration-source peak centroids in a unified manner. These were coupled with transition-energy data gleaned from the literature. ROOT fits the centroids and energies, and the energy calibration is obtained with precise uncertainty for the fit parameters. As we utilized higher order polynomials, the fit quality improved. As a result, we employed the cubic fit to calibrate the energy.

The propagation of error from the defining energy calibration equation takes all errors into account by the formula given as follows:

$$\sigma_E^2 = \sum_{i=0}^{3}\left(\frac{\partial E}{\partial a_i}\right)^2\sigma_{a_i}^2 + 2\sum_{i=0}^{3}\sum_{j>i}^{3}\left(\frac{\partial E}{\partial a_i}\right)\left(\frac{\partial E}{\partial a_j}\right)\mathrm{cov}_{ij} + \left(\frac{\partial E}{\partial ch}\right)^2\sigma_{ch}^2$$
$$= \sum_{i=0}^{3}\left(\frac{\partial E}{\partial a_i}\right)^2\sigma_{a_i}^2 + 2\sum_{i=0}^{3}\sum_{j>i}^{3}\left(\frac{\partial E}{\partial a_i}\right)\left(\frac{\partial E}{\partial a_j}\right)\mathrm{cor}_{ij}\sigma_i\sigma_j + \left(\frac{\partial E}{\partial ch}\right)^2\sigma_{ch}^2. \quad (1)$$

Here, σ_{a_i} is the error of the fit parameters, cov_{ij} and cor_{ij} are covariance and correlation and σ_{ch} is the errors of the centroid. The energy and uncertainty were calculated according to Eq. (1) and are listed in Table 3.

The measurement of the half-life has involved the measurement of the decay as a function of time and the fit to the activity with the exponential decay curve. Obtaining half-life from the peak data, integration of the activity in equal-size time step has been performed by

$$C(T) = \int_{T-\Delta T}^{T+\Delta T} A(t)dt = C_0 e^{-\lambda T}(e^{\lambda\Delta T} - e^{-\lambda\Delta T}), \quad (2)$$

where T is the time for counting, ΔT is constant and $C_0 = A_0/\lambda$. this can be performed by taking independent spectra of length ΔT and restarting the count at the end of each time step. The errors of the counts obtained in this way are independent of each other because the counts obtained in two consecutive spectra are not correlated with each other. The logarithm of Eq. (2) was used for fitting and a simple linear was performed in order to obtain λ. By using the decay constant λ, half-life was obtained for ^{47}Sc.

3. Results and Discussion

All possible reactions in this experiment have been given in Table 2. The stable titanium isotopes created via photo-neutron reaction have not been given because they do not contribute to the gamma-ray spectrum. As can be seen in the table only ^{45}Sc isotope has been generated via photo-neutron reaction after the electron capture process of ^{45}Ti ($T_{1/2} = 184.8$ min). There is no gamma-ray peak observed from this isotope since the decay goes directly to the ground state of ^{45}Sc with 99.685% branching intensity.[32]

Table 2. Possible reaction paths after gamma activation of the titanium target.

Produced isotope	Reaction
^{45}Sc	$^{46}\mathrm{Ti} + \gamma \rightarrow ^{45}\mathrm{Ti} + \mathrm{n}$
	$^{45}\mathrm{Ti} + \mathrm{e} + \nu \rightarrow ^{45}\mathrm{Sc}^{*}$
	$^{45}\mathrm{Sc}^{*} \rightarrow ^{45}\mathrm{Sc} + \gamma$
^{46}Ti	$^{47}\mathrm{Ti} + \gamma \rightarrow ^{46}\mathrm{Sc} + \mathrm{p}$
	$^{46}\mathrm{Sc} \rightarrow ^{46}\mathrm{Ti}^{*} + \mathrm{e} + \nu^{-}$
	$^{46}\mathrm{Ti}^{*} \rightarrow ^{46}\mathrm{Ti} + \gamma$
^{47}Ti	$^{48}\mathrm{Ti} + \gamma \rightarrow ^{47}\mathrm{Sc} + \mathrm{p}$
	$^{47}\mathrm{Sc} \rightarrow ^{47}\mathrm{Ti}^{*} + \mathrm{e} + \nu^{-}$
	$^{47}\mathrm{Ti}^{*} \rightarrow ^{47}\mathrm{Ti} + \gamma$
^{48}Ti	$^{49}\mathrm{Ti} + \gamma \rightarrow ^{48}\mathrm{Sc} + \mathrm{p}$
	$^{48}\mathrm{Sc} \rightarrow ^{48}\mathrm{Ti}^{*} + \mathrm{e} + \nu^{-}$
	$^{48}\mathrm{Ti}^{*} \rightarrow ^{48}\mathrm{Ti} + \gamma$
^{49}Ti	$^{50}\mathrm{Ti} + \gamma \rightarrow ^{49}\mathrm{Sc} + \mathrm{p}$
	$^{49}\mathrm{Sc} \rightarrow ^{49}\mathrm{Ti}^{*} + \mathrm{e} + \nu^{-}$
	$^{49}\mathrm{Ti}^{*} \rightarrow ^{49}\mathrm{Ti} + \gamma$

All titanium isotopes which can contribute to the gamma-ray spectrum have been generated via photo-proton reactions. ^{46}Sc ($T_{1/2}$ = 83.79 d) isotope decays to 4^{+} state of ^{46}Ti isotope with 2009.8 keV energy. It should be noted that all of the spin and parity assignments are based on literature and are not extracted from the data collected in this experiment. The excited titanium isotope emits gamma-rays to reach the ground state. The gamma-rays from this isotope measured in this study are 889.259 keV and 1120.489 keV. 2010 keV direct transition from 4^{+} state to ground state has not been identified due to its very weak intensity ($\sim 10^{-5}$). ^{47}Sc ($T_{1/2}$ = 3.35 d) isotope decays to $7/2^{-}$ state of ^{47}Ti isotope. The gamma-ray from this isotope has been measured as 159.417 keV as the most intense peak in the gamma-ray spectrum due to ^{47}Sc is formed from the most abundant ^{48}Ti isotope. ^{48}Sc isotope decays to one of the 6^{+} states of ^{48}Ti isotope with 3333.2 or 3508.6 keV energies. The gamma-rays from the de-excitation in this isotope have been measured as 983.805 keV from 2^{+} to 0^{+} transition, 1037.621 from 6^{+} to 4^{+} transition and 1312.145 keV from 4^{+} to 2^{+} transition.

In the last energetically favorable reaction, the formed ^{49}Sc isotope decays to directly (99.940% branching) ^{49}Ti ground state. Therefore, we could not see any gamma-rays from this isotope in the spectrum. In Table 3, we have summarized all observed gamma-rays in this study with their standard deviations and compared with the available literature values.[25]

Once the peak position has been established the change in the count rate under the peak can be used to determine the half-life of the unstable nuclei. The spectrum was transformed to many spectra of the same time length. The change in the count at each time step has the same exponential dependence as the activity $N(t) = N_0 e^{-\lambda t}$. For the determination of the half-life of ^{47}Sc isotope, the peak of

Table 3. List of observed and literature transition energies[25] of $^{46-48}$Ti isotopes with the error values.

Nuclei	Path	Energy (keV)	Literature energy (keV)
^{46}Ti	2^+ to 0^+	889.26(3)	889.277(3)
	4^+ to 2^+	1120.49(2)	1120.545(4)
^{47}Ti	$7/2^-$ to $5/2^-$	159.417(6)	159.373(12)
^{48}Ti	2^+ to 0^+	983.80(9)	983.5299(24)
	6^+ to 4^+	1037.62(10)	1037.599(26)
	4^+ to 2^+	1312.14(10)	1312.103(5)

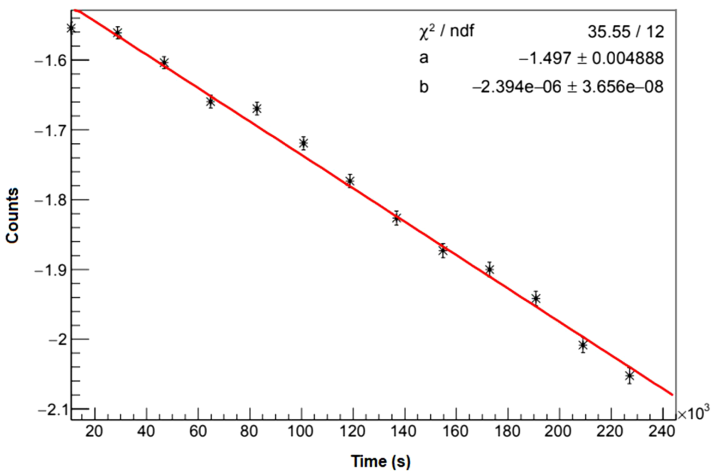

Fig. 3. The decay curve of the counts in the peaks reflects the decay of the unstable ^{47}Sc isotope.

159.417 keV has been chosen for the investigation (Fig. 3), which is the most intense peak. In the fitting process, decay constant (λ) has been obtained as 2.395×10^{-6} (4.876×10^{-8}) which corresponds to 3.35(12) days half-life. The literature value is 3.3492(6) days.

4. Conclusions

The photonuclear reaction performed on titanium isotopes in the giant-dipole-resonance region has been studied. For this purpose, bremsstrahlung photons, whose spectrum has the endpoint energy of 18 MeV, have been used. The gamma energy transitions of the decays were measured with good accuracy. The residual activity of the sample material has been measured via HPGe detectors. ^{47}Sc is observed to be produced as the most abundant product by irradiation of natural titanium and the observed results have been compared with the adopted literature values. Our results are consistent with the other experiments as can be seen in Table 3. These results increase our knowledge of a nucleus of relevance for the production of radioactive isotopes in medical applications. Additionally, in this study, our aim

was not only obtaining more sensitive and accurate energy values for the transitions in the isotopes, but also to show the usefulness of this relatively basic method and to show a clinical linac is well suited for such fundamental studies. Besides, the measured transitions confirm the corresponding reference data from the literature.

Acknowledgments

This work was supported by Erciyes University Scientific Research Center Project Number FBA-2014-5224. The authors G. Koçak and S. Akkoyun specially thank the Akdeniz University Nuclear Research and Application Center.

References

1. C. Segebade, H. P. Weise and G. J. Lutz, *Photon Activation Analysis* (Walter de Gruyter, Berlin, Germany, 1987).
2. K. Strauch, *Annu. Rev. Nucl. Sci.* **2** (1953) 105.
3. IAEA-TECDOC-1178, *Handbook on Photonuclear Data for Applications*: *Cross-Sections and Spectra* (Nuclear Data Section, IAEA, Vienna, Austria, 2000).
4. J. Chadwick and M. Goldhaber, *Nature* **134** (1934) 237.
5. J. Green, S. Zaijing, D. Wells and H. Maschner, *Proc. AIP* **1336** (2011) 497.
6. Y. O. Lee, T. Fukahori and J. Chang, *J. Nucl. Sci. Technol.* **35** (1998) 685.
7. Z. J. Sun, D. P. Wells, C. Segebade, H. Maschner and B. Benson, *J. Radioanal. Nucl. Chem.* **296** (2013) 293.
8. K. Wagner, W. Gorner, M. Hedrich, P. Jost and C. Segebade, *Fresenius' J. Anal. Chem.* **362** (1998) 382.
9. M. S. Johnson *et al.*, *Journal of the Korean Physical Society* **59**(2) (2011) 1414–1417.
10. Z. Randa, J. Kucera, J. Mizera and J. Frana, *J. Radioanal. Nucl. Chem.* **271** (2007) 589.
11. T. R. Sherwood and W. E. Turchinetz, *Nucl. Phys.* **29** (1962) 292.
12. S. Oikawa and K. Shoda, *Nucl. Phys. A* **277** (1977) 301.
13. M. N. Thompson *et al.*, *Res. Rep. Lab. Nucl. Sci. Tohoku Univ.* **10** (1977) 55.
14. J. Weise *et al.*, *Res. Rep. Lab. Nucl. Sci. Tohoku Univ.* **11** (1978) 43.
15. R. E. Pywell and M. N. Thompson, *Nucl. Phys. A* **318** (1979) 461.
16. R. E. Pywell, M. N. Thompson and R. A. Hicks, *Nucl. Phys. A* **325** (1979) 116.
17. R. Sutton *et al.*, *Nucl. Phys. A* **339** (1980) 125.
18. M. Mayir, F. Harmon and V. N. Starovoitova, *Appl. Radiat. Isot.* **102** (2015) 1.
19. D. A. Rotsch *et al.*, *Appl. Radiat. Isot.* **131** (2018) 77.
20. P. Mohr, S. Brieger, G. Witucki and M. Maetz, *Nucl. Instrum. Methods Phys. Res. A*, *Accel. Spectrom. Detect. Assoc. Equip.* **580** (2007) 1201.
21. M. Tatari and A. H. Ranjbar, *Ann. Nucl. Energy* **63** (2014) 69.
22. M. Roig, V. Panettieri, M. Ginjaume and A. Sanchez-Reyes, *Phys. Med. Biol.* **49** (2004) N243.
23. J. H. Chao, M. T. Liu, S. A. Yeh, S. S. Huang, J. M. Wu, D. Y. L. Chang, F. Y. Hsu, C. Y. Chuang, H. Y. Liu and Y. C. Sun, *Appl. Radiat. Isot.* **67** (2009) 1121.
24. T. Fujibuchi, S. Obara, H. Sato, M. Nakajima, N. Kitamura, T. Sato, H. Kumada, T. Sakae and T. Fujisaki, *Prog. Nucl. Sci. Technol.* **2** (2011) 803.
25. A. Alfuraih, M. P. W. Chin and N. M. Spyrou, *J. Radioanal. Nucl. Chem.* **278** (2008) 681.

26. I. Boztosun, H. Dapo, M. Karakoc, S. Ozmen, Y. Cecen, A. Coban, T. Caner, E. Bayram, T. Saito, T. Akdogan, V. Bozkurt, Y. Kucuk, D. Kaya and M. Harakeh, *Eur. Phys. J. Plus* **130** (2015) 185.
27. I. Boztosun, H. Dapo and M. Karakoc, *Mod. Phys. Lett. A* **31** (2016) 1650212.
28. S. Akkoyun, T. Bayram, F. Dulger, H. Dapo and I. Boztosun, *Int. J. Mod. Phys. E* **25** (2016) 1650045.
29. C. Eke, I. Boztosun, H. Dapo, C. Segebade and E. Bayram, *J. Radioanal. Nucl. Chem.* **309** (2016) 79.
30. D. Radford, *Nucl. Instrum. Methods Phys. Res. A*, *Accel. Spectrom. Detect. Assoc. Equip.* **361** (1995) 297.
31. R. Brun and F. Rademakers, *Nucl. Instrum. Methods Phys. Res. A*, *Accel. Spectrom. Detect. Assoc. Equip.* **389** (1997) 81.
32. NUDAT (2019). https://www.nndc.bnl.gov/nudat2/.